EUROPEAN ORGANIZATION FOR NUCLEAR RESEARCH

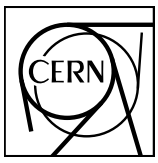

CERN-PH-EP-2016-046
29 February 2016

Centrality dependence of ψ(2S) suppression in p-Pb collisions at $\sqrt{s_{\rm NN}}$ = 5.02 TeV

ALICE Collaboration*

Abstract

The inclusive production of the $\psi(2S)$ charmonium state was studied as a function of centrality in p-Pb collisions at the nucleon-nucleon center of mass energy $\sqrt{s_{\rm NN}}$ = 5.02 TeV at the CERN LHC. The measurement was performed with the ALICE detector in the center of mass rapidity ranges $-4.46 < y_{\rm cms} < -2.96$ and $2.03 < y_{\rm cms} < 3.53$, down to zero transverse momentum, by reconstructing the $\psi(2S)$ decay to a muon pair. The $\psi(2S)$ production cross section $\sigma_{\psi(2S)}$ is presented as a function of the collision centrality, which is estimated through the energy deposited in forward rapidity calorimeters. The relative strength of nuclear effects on the $\psi(2S)$ and on the corresponding 1S charmonium state J/ψ is then studied by means of the double ratio of cross sections $[\sigma_{\psi(2S)}/\sigma_{J/\psi}]_{\rm pPb}/[\sigma_{\psi(2S)}/\sigma_{J/\psi}]_{\rm pp}$ between p-Pb and pp collisions, and by the values of the nuclear modification factors for the two charmonium states. The results show a large suppression of $\psi(2S)$ production relative to the J/ψ at backward rapidity, corresponding to the flight direction of the Pb-nucleus, while at forward rapidity the suppressions of the two states are comparable. Finally, comparisons to results from lower energy experiments and to available theoretical models are presented.

*See Appendix A for the list of collaboration members

1 Introduction

Charmonia are bound states of a charm and an anticharm quark ($c\overline{c}$), and represent an important testing ground for the properties of the strong interaction. In high-energy proton-proton collisions, the charmonium production process is usually factorized in two steps: the creation of a $c\overline{c}$ pair via hard gluon fusion followed, on a longer time scale, by the binding and emission of one or more gluons that brings the pair to a colour singlet state. This process is described reasonably by theoretical models inspired by Quantum Chromodynamics (QCD) [1], although a quantitative evaluation of the production cross sections and polarization of the charmonium states still meets difficulties [1,2].

If a charmonium state is produced within the nuclear medium, as can happen in proton-nucleus collisions, several effects become important and might influence the charmonium formation. In particular, the modification in the nucleus of the parton distribution functions, known as nuclear shadowing [3–5], can lead to a suppression or an enhancement of the charmonium production. Furthermore, the incoming gluons, as well as the outgoing $c\overline{c}$ pair, may lose energy in the nuclear medium, altering the differential distributions of the produced charmonium state [6]. Finally, once the bound state is formed, it may be dissociated via collisions within nuclear matter [7–9]. However, the formation of the final-state resonance occurs in a finite time $\tau_{\rm f}$ which, depending on the kinematics of the $c\overline{c}$ pair and on the collision energy, may be longer than its crossing time, $\tau_{\rm c}$, in the nucleus.

Among the narrow charmonium states, i.e. those with a mass smaller than twice the mass of the lightest D mesons, we address in this paper the vector states ($J^{PC} = 1^{--}$) J/ψ, characterized by a binding energy $\Delta E \sim 650$ MeV (corresponding to the mass gap to the open charm threshold), and the weakly bound ψ(2S), with $\Delta E \sim 50$ MeV [10]. A comparison of the production cross section of the two states in proton-nucleus collisions offers interesting insights into the size of the various cold nuclear matter (CNM) effects outlined above. In particular, shadowing acts on the initial state partons and affects in a very similar way the production of the two charmonium states. Also the energy loss mechanism was shown to be largely independent of the final resonance [6]. On the contrary, the break-up probability of the final resonance inside the nucleus should be much larger for the weakly bound ψ(2S) [11].

Early results on J/ψ and ψ(2S) production in proton-nucleus collisions were obtained at fixed target experiments by E866 [12] at FNAL ($\sqrt{s_{\rm NN}} = 63$ GeV), by HERA-B [13] at HERA ($\sqrt{s_{\rm NN}} = 39$ GeV) and by NA38, NA50, NA60 [14–16] at the CERN SPS ($\sqrt{s_{\rm NN}} = 17 - 29$ GeV). At mid-rapidity, i.e., close to $y_{\rm cms} = 0$, the relative production cross section $\sigma_{\psi(2S)}/\sigma_{J/\psi}$ was found to decrease rather strongly for increasing mass number of the nuclear target. Since part of the kinematic domain accessed at fixed target energies is characterized by $\tau_{\rm f} < \tau_{\rm c}$ [9], such an observation can indeed be related to a stronger break-up effect on the weakly bound ψ(2S).

At collider energies, it becomes technically more difficult to have data samples corresponding to various nuclear colliding species. Therefore, in order to vary the thickness of CNM crossed by the $c\overline{c}$ pair, one can rather select classes of events based on estimators of the geometry (centrality) of the collision, corresponding to various ranges in the number of nucleon-nucleon collisions $N_{\rm coll}$. This procedure was followed by the PHENIX experiment at RHIC, which studied the nuclear modification factors, defined as the ratio between the measured yields in d-Au and proton-proton collisions, normalized to $N_{\rm coll}$, for the J/ψ and ψ(2S) resonances at mid-rapidity [17]. At $\sqrt{s_{\rm NN}} = 200$ GeV, the nuclear modification factors were smaller by a factor ~ 3 for ψ(2S) relative to J/ψ for central events, indicating a stronger suppression for ψ(2S). However, such an observation is surprising since for mid-rapidity production at RHIC energies the time spent by the $c\overline{c}$ pair in the nucleus ($\tau_{\rm c} < 0.05$ fm/c) is below the formation time of the final-state resonance (most theory estimates [9,18,19] give $\tau_{\rm f} > 0.15$ fm/c). In such a situation, one would rather expect a similar suppression for the J/ψ and ψ(2S) states.

At the LHC, centrality-integrated results on the ψ(2S) and J/ψ resonances for p-Pb collisions at $\sqrt{s_{\rm NN}} =$ 5.02 TeV were obtained by ALICE [20,21] and LHCb [22,23]. At both forward and backward rapidities,

corresponding to the p-going and Pb-going directions respectively, a significantly larger suppression of $\psi(2S)$ compared to J/ψ was observed, relative to proton-proton collisions. Again, this result was unexpected, as the τ_c values are either at most the same order of magnitude (at negative y_{cms}) or more than two orders of magnitude smaller (at positive y_{cms}) than τ_f [20].

As outlined above, a differential measurement as a function of the collisions centrality is equivalent to a study of the propagation of the $c\overline{c}$ pairs over various thicknesses of CNM. In this Letter, we go in that direction by showing results obtained by the ALICE Collaboration on $\psi(2S)$ studies in p-Pb collisions as a function of centrality, estimated through the energy deposited at very forward rapidity by the remnants of the Pb-nucleus. The corresponding J/ψ studies were published in [24]. In Sect. 2 we give a brief overview of the experimental apparatus and run conditions. Sect. 3 presents details on the analysis procedure, while Sect. 4 is dedicated to the results. The conclusions are presented in Sect. 5.

2 Experimental conditions

The analysis presented in this Letter is based on the detection of the $\psi(2S) \to \mu^+\mu^-$ decay in the forward muon spectrometer of ALICE, described in detail elsewhere [25, 26]. This detector covers the pseudorapidity range $-4 < \eta_{lab} < -2.5$ and includes a 3 T· m dipole magnet and five stations of tracking chambers, the central one being inside the magnet gap. A main absorber (10 interaction lengths thick) is positioned between the ALICE interaction point and the tracking system, in order to remove hadrons. A second absorber is placed downstream of the tracking detectors. It removes the remaining hadrons and low-momentum muons produced predominantly from π and K decays, and is followed by two stations of trigger chambers that select muon candidates based on their transverse momentum (p_T). In addition to the muon spectrometer, the first two layers of the Inner Tracking System (SPD, i.e., Silicon Pixel Detectors, the first covering $|\eta_{lab}| < 2.0$ and the second $|\eta_{lab}| < 1.4$) [27] are used for the determination of the position of the interaction vertex. The two V0 scintillator hodoscopes (covering $-3.7 < \eta_{lab} < -1.7$ and $2.8 < \eta_{lab} < 5.1$, respectively) are used for triggering purposes [28]. Finally, two sets of Zero-Degree Calorimeters (ZDC), positioned at 112.5 m on the two sides of the interaction point, each one including a neutron calorimeter (ZN) and a proton calorimeter (ZP), are used to clean-up the event sample from interactions occurring out of the nominal bunches and for the centrality estimate [29, 30].

The data-taking conditions were described in [21,31] and are briefly stated here. Two data samples were taken, corresponding to the p-beam or the Pb-beam going in the direction of the muon spectrometer, and labelled in the following as p-Pb and Pb-p, respectively. The integrated luminosities were $L_{int}^{pPb} = 5.01 \pm 0.19$ nb^{-1} and $L_{int}^{Pbp} = 5.81 \pm 0.20$ nb^{-1} [32]. The events used in this analysis were collected requiring a coincidence between a minimum bias (MB) trigger condition, defined by the logical AND of signals on the two V0 hodoscopes (>99% efficiency for non-single diffractive events), and the detection of two candidate opposite-sign tracks in the trigger system of the muon spectrometer. A $p_T^{\mu} > 0.5$ GeV/c cut on such tracks was also imposed at the trigger level. The offline event selection, the muon reconstruction and identification criteria and the kinematic and quality cuts applied at the single-muon and dimuon levels have already been described in Refs. [20, 21, 24, 33]. In particular, the covered dimuon rapidity ranges were $2.03 < y_{cms} < 3.53$ and $-4.46 < y_{cms} < -2.96$ for the p-Pb and Pb-p configurations, respectively.

3 Data analysis

In this Section, the evaluation of the various elements that enter the cross section measurements and the nuclear modification factor calculations are described.

The centrality selection and the determination of N_{coll} are based on a hybrid method described in detail in Ref. [30]. Events are selected according to the energy deposited at very large rapidity in the ZN positioned in the Pb-going direction, which mainly detects slow neutrons emitted by the Pb-nucleus as

the result of the interaction. Their emission, according to results obtained in the analysis of lower energy proton-nucleus experiments, is expected to be monotonically related to $N_{\rm coll}$ [34]. A centrality selection based on the ZN energy is found to be less biased than other centrality estimators, based on the charged particle multiplicity measurements at central (SPD) or forward (V0) pseudorapidity [30]. The average number of nucleon-nucleon collisions $\langle N_{\rm coll}\rangle$ for each ZN-selected centrality class is then obtained by assuming that the charged particle multiplicity measured at central rapidity is proportional to the number of participants $N_{\rm part} = N_{\rm coll} + 1$ [35]. The values of $\langle N_{\rm coll}\rangle$, used in this analysis, are reported in Tab. 1, together with their uncertainties.

ZN centrality class	$\langle N_{\rm coll}\rangle$
2–20%	$11.3 \pm 0.6 \pm 0.9$
20–40%	$9.6 \pm 0.2 \pm 0.8$
40–60%	$7.1 \pm 0.3 \pm 0.6$
60–80%	$4.3 \pm 0.3 \pm 0.3$
80–100%	$2.1 \pm 0.1 \pm 0.2$

Table 1: Average numbers of binary nucleon-nucleon collisions, $N_{\rm coll}$, evaluated in the ZN centrality classes used in this analysis. The first quoted systematic uncertainty is uncorrelated, while the second is global.

The centrality classes used in this analysis correspond to 2–20%, 20–40%, 40–60%, 60–80% and 80–100% of the measured cross section corresponding to the MB trigger. Very central events (0–2%) are discarded from the event sample due to a large contamination from pile-up interactions.

The estimate of the $\psi(2S)$ signal is based on fits to the dimuon invariant mass spectra $m_{\mu\mu}$ corresponding to events in the centrality ranges defined above. Details on the procedure, on the fitting functions and on the estimate of systematic uncertainties are discussed in [20]. The function used in the fit is the sum of a continuum background, mainly related to uncorrelated decays from pions and kaons and to semi-leptonic decays of pairs of hadrons with open heavy flavor, and of resonance shapes corresponding to the J/ψ and $\psi(2S)$ mesons. The background is parameterized by various empirical shapes, directly fitted to the data. The resonances are described by either a Crystal Ball function or a pseudo-gaussian with a mass-dependent width [36]. The main parameters of the J/ψ line shapes, i.e. mass position and width, are left as free parameters, while the non-gaussian tail parameters are fixed to Monte-Carlo (MC) estimates. The $\psi(2S)$ line shape parameters, given the less favourable signal over background, are fixed relative to those of the J/ψ, assuming that the mass difference and the widths scale according to the MC result. The results of the fits are shown in Fig. 1.

The quality of the fits is good, with χ^2/ndf ranging from 0.7 to 1.3. The $\psi(2S)$ signal is visible in all the centrality bins, and the signal over background ratio increases from central (0.06 for p-Pb and 0.04 for Pb-p) to peripheral events (0.15 and 0.28, respectively). The number of reconstructed $\psi(2S)$ for the various centrality bins, $N^i_{\psi(2S)\to\mu^+\mu^-}$, ranges from $265 \pm 73 \pm 32$ (i= 2–20%) to $100 \pm 29 \pm 9$ (i= 80–100%) in p-Pb, where the first uncertainty is statistical and the second one is systematic. The corresponding values for Pb-p are $141 \pm 64 \pm 13$ (i= 2–20%) and $65 \pm 20 \pm 7$ (i= 80–100%). The systematic uncertainties on the signal extraction are given by the root mean square of the number of $\psi(2S)$ obtained with various fits corresponding to different fitting functions for background and signal, and by varying the non-gaussian tails of the resonance shape, and the $\psi(2S)$ mass resolution values. In p-Pb, the systematic uncertainties range between 9 and 12% from peripheral to central events (9–20% for Pb-p).

The product of acceptance times efficiency $A \times \varepsilon$ for the $\psi(2S)$ resonance was calculated with the MC-based procedure described in Refs. [20, 21]. The values are the same as quoted there for the centrality integrated production (0.270 ± 0.014 for p-Pb and 0.184 ± 0.013 for Pb-p), since it was verified that the tracking efficiency does not depend on the centrality of the collision [24]. The quoted errors are the quadratic sum of the systematic uncertainties on tracking, trigger and matching efficiencies and on the choice of the $\psi(2S)$ $p_{\rm T}$ and y input shapes used in the MC simulations.

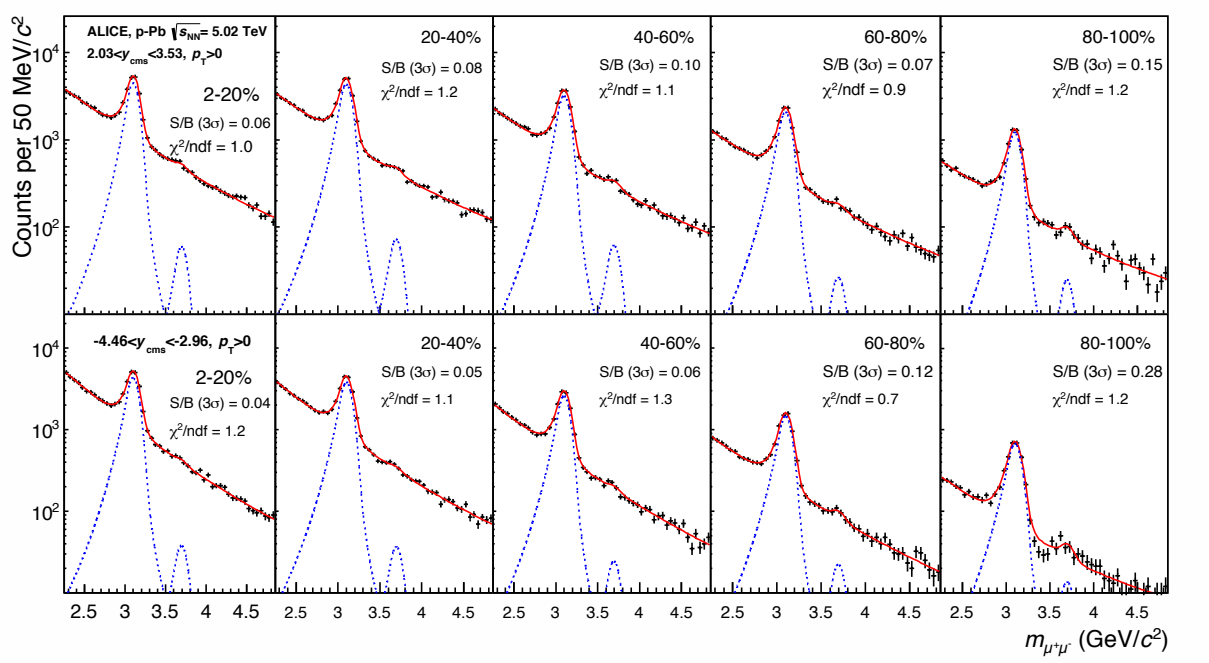

Fig. 1: Opposite-sign dimuon invariant mass spectra in ZN centrality classes at forward (top) and backward (bottom) rapidities. The fit curves shown in red in the figure correspond to the sum of signal and background shapes, the former being also shown separately in blue.

The normalization of the $\psi(2S)$ yield was calculated according to the procedure described in Ref. [24]. It is based on the evaluation, for each centrality class, of the number of minimum bias events as $N^i_{\rm MB} = F^i \cdot N^i_{\rm DIMU}$, where $N^i_{\rm DIMU}$ is the number of dimuon-triggered events and F^i is the inverse of the probability of having a dimuon triggered in a MB event for that class. The F^i-values increase from central to peripheral events and are 287 ± 3 and 694 ± 8 for the 2–20% centrality class in p-Pb and Pb-p respectively. The corresponding values for the 80–100% class are 3291 ± 36 and 3338 ± 35. The systematic uncertainties quoted above (statistical uncertainties are negligible) come from the comparison obtained with two slightly different approaches in the calculation of F^i, as detailed in [24].

In the evaluation of the systematic uncertainties on F^i, the presence of interaction pile-up was considered. Pile-up can lead to a bias in the evaluation of the centrality of the collision since, for example, the superposition of the signals from two peripheral events in the ZN can fake a more central event. The contribution of pile-up was calculated by detecting events with multiple interaction vertices in the SPD, and checking via a fast Monte-Carlo that the ZN energy distribution can be reproduced assuming a pile-up probability corresponding to the observed interaction rate. Events in the 0–2% centrality interval were rejected, as the pile-up contribution becomes significant ($\sim$30%) in that region. The effect is small but not negligible in the 2–20% range, where it amounts to 2.1% (2.6%) for p-Pb (Pb-p), and becomes $< 1\%$ going towards more peripheral events.

From the quantities described above, the inclusive cross section for $\psi(2S)$ production in the centrality bin i, times its branching ratio to dimuons B.R.$_{\psi(2S)\to\mu\mu}$, was calculated with the following expression

$$\text{B.R.}_{\psi(2S)\to\mu^+\mu^-}\,\sigma^{i,\psi(2S)}_{\rm pPb} = \frac{N^i_{\psi(2S)\to\mu^+\mu^-}}{(A\times\varepsilon)\cdot N^i_{\rm MB}} \times \sigma_{\rm MB} \qquad (1)$$

The ratio $N_{\rm MB}/\sigma_{\rm MB}$, where $N_{\rm MB}$ is the total number of minimum bias events and $\sigma_{\rm MB}$ is the cross section for events satisfying the minimum bias trigger condition, gives the integrated luminosity $L_{\rm int}$. The $\sigma_{\rm MB}$ values were evaluated through a van der Meer scan which gives $\sigma^{\rm pPb}_{\rm MB} = 2.09 \pm 0.07$ b and

$\sigma_{\rm MB}^{\rm Pbp} = 2.12 \pm 0.07$ b [32]. A determination of the luminosity which makes use of a different reference process, based on the signals released in a Čerenkov counter [26], gives a result compatible within 1% [32]. Therefore, an additional 1% uncertainty is added to the $\sigma_{\rm MB}$ values used in the ψ(2S) cross section determination.

The comparison of the ψ(2S) and J/ψ production cross sections can be performed by calculating the ratio $\mathrm{B.R.}_{\psi(\rm 2S)\to\mu^+\mu^-}\sigma_{\psi(\rm 2S)}/\mathrm{B.R.}_{\rm J/\psi\to\mu^+\mu^-}\sigma_{\rm J/\psi}$. In this way, the uncertainties related to the cross section normalization and to the reconstruction efficiency cancel out. The J/ψ cross section values that enter this ratio are those reported in [24], with the value for the centrality interval 2–20% obtained by summing the 2–10% and 10–20% results. This ratio can be further normalized to the corresponding measurement in pp collisions. This quantity, called double ratio in the following, gives direct access to modifications in the ψ(2S) production relative to that of the J/ψ, going from pp to p-Pb collisions. Due to the lack of precise pp data at $\sqrt{s} = 5.02$ TeV, the results obtained at $\sqrt{s} = 7$ TeV [37] were used instead. This choice is justified from the fact that the $\sqrt{s}$- and y-dependence of the cross section ratio is known to be weak in the TeV beam energy range. An 8% systematic uncertainty has been included, corresponding to the maximum estimated size of the variation of the ratio between the two energies [20].

The estimate of the nuclear modification factors $Q_{\rm pPb}^{i,\psi(2S)}$ as a function of centrality is performed as the product of the corresponding $Q_{\rm pPb}^{i,\rm J/\psi}$ for the J/ψ [24] (except for the 2–20% centrality interval where $Q_{\rm pPb}^{i,\rm J/\psi}$ was re-computed by merging the 2–10% and 10–20% bins) and the double ratio between the ψ(2S) and J/ψ cross sections in p-Pb and pp collisions:

$$Q_{\rm pPb}^{i,\psi(\rm 2S)} = Q_{\rm pPb}^{i,\rm J/\psi} \cdot \frac{\sigma_{\rm pPb}^{i,\psi(\rm 2S)}}{\sigma_{\rm pPb}^{i,\rm J/\psi}} \cdot \frac{\sigma_{\rm pp}^{\rm J/\psi}}{\sigma_{\rm pp}^{\psi(\rm 2S)}} \tag{2}$$

The uncertainties are obtained combining those on $Q_{\rm pPb}^{i,\rm J/\psi}$ [24] with those on the double ratio, avoiding a double counting of the J/ψ related uncertainties. The notation $Q_{\rm pPb}^{i,\psi(2S)}$, rather than the more usual $R_{\rm pPb}^{i,\psi(2S)}$, is used in this Letter, to draw attention to possible residual biases in the centrality determination, related to the loose correlation between the centrality estimators and the corresponding collision geometry [30].

Table 2 summarizes the values of the systematic uncertainties on the various ingredients that enter the cross section determination and the calculation of the nuclear modification factor.

Source of uncertainty	$\sigma_{\rm pPb}^{\psi(\rm 2S)}$, $Q_{\rm pPb}^{\psi(\rm 2S)}$ 2.03$<y_{\rm cms}<$3.53	$\sigma_{\rm Pbp}^{\psi(\rm 2S)}$, $Q_{\rm Pbp}^{\psi(\rm 2S)}$ -4.46$<y_{\rm cms}<$-2.96
Tracking efficiency (I)	4	6
Trigger efficiency (I)	3	3.4
Matching efficiency (I)	1	1
Signal extraction	10.8 − 13.4	10.8 − 20.9
MC input	1.8	1.8
$\sigma_{\rm MB}$ (I)	3.3	3.0
$\sigma_{\rm MB}$ (I,II)	1.6	1.6

Table 2: Systematic uncertainties, in percentage, on the ψ(2S) cross sections and nuclear modification factors. For centrality-dependent quantities, the range of variation is given. Type I uncertainties are correlated over centrality, while type II are correlated between the forward and the backward rapidity regions. When no indication is given, the uncertainties are uncorrelated. The uncertainty on $\sigma_{\rm MB}$ is related to the ψ(2S) cross section only.

4 Results

The $\psi(2S)$ production cross sections as a function of the centrality of the collision, expressed via $\langle N_{\rm coll}\rangle$, are plotted in Fig. 2 (left). As expected, their values increase with $\langle N_{\rm coll}\rangle$.

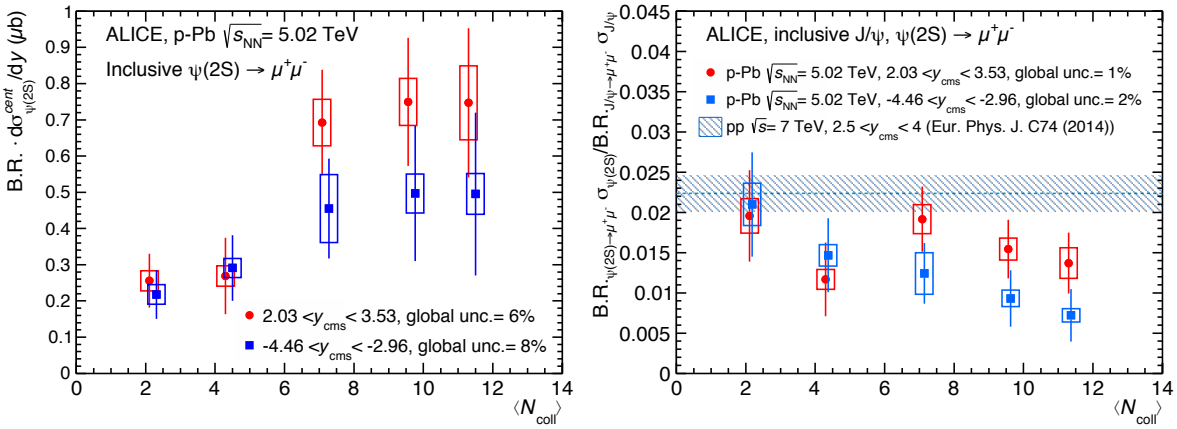

Fig. 2: Left: $\psi(2S)$ production cross sections shown as a function of $\langle N_{\rm coll}\rangle$ for both p-Pb and Pb-p collisions. Right: $\mathrm{B.R.}_{\psi(2S)\to\mu^+\mu^-}\sigma_{\psi(2S)}/\mathrm{B.R.}_{J/\psi\to\mu^+\mu^-}\sigma_{J/\psi}$ shown as a function of $\langle N_{\rm coll}\rangle$ and compared to the pp value (line), with a band representing its uncertainty. In both figures, vertical error bars correspond to statistical uncertainties, while the open boxes represent the systematic uncertainties. The Pb-p points are slightly shifted in $\langle N_{\rm coll}\rangle$ to improve visibility.

In Fig. 2 (right) the ratio $\mathrm{B.R.}_{\psi(2S)\to\mu^+\mu^-}\sigma_{\psi(2S)}/\mathrm{B.R.}_{J/\psi\to\mu^+\mu^-}\sigma_{J/\psi}$ is shown as a function of $\langle N_{\rm coll}\rangle$ and compared with the corresponding value for pp collisions. Despite the large uncertainties, the data suggest a decreasing trend from peripheral to central events, in particular at backward rapidity, indicating a suppression of the $\psi(2S)$ production relative to the J/ψ. While for peripheral collisions the cross section ratios are consistent with the pp value, they become a factor 2–3 smaller for central events, in both rapidity ranges. As remarked in Sect. 3, the pp cross section ratio measured at $\sqrt{s} = 7$ TeV has been used, including an 8% additional uncertainty to account for its possible $\sqrt{s}$- and y-dependence.

The degree of suppression of $\psi(2S)$ is directly quantified in Fig. 3 where the double ratio between the $\psi(2S)$ and J/ψ cross sections in p-Pb and pp collisions is shown. The result is compared with two theoretical calculations. The first is based on a scenario where the resonances may be dissociated via interactions with the partons or hadrons produced in the collision in the same rapidity region (co-movers) [38]. The model includes contributions from nuclear shadowing, based on the EPS09 LO parameterization [3], and a co-mover interaction term, with dissociation cross sections $\sigma^{\mathrm{co-J/\psi}} = 0.65$ mb and $\sigma^{\mathrm{co-\psi(2S)}} = 6$ mb, these values being fixed from fits to low-energy experimental data [39]. The effect of co-movers is larger at backward rapidity since their density is larger in that region. The calculated co-mover densities are compatible with the measured experimental charged particle multiplicities [40]. The calculation reproduces well the measured values of the double ratio. Shadowing effects are very similar for the two mesons and in this model they are assumed to cancel out in the double ratio, so that only co-mover absorption plays a role. The second model (QGP+HRG) is based on a thermal-rate equation framework [41] which also implements the dissociation of charmonia in a hadron resonance gas, including a total of 52 non-strange and single-strange meson species, up to a mass of 2 GeV/c^2 [42]. The fireball evolution includes the transition from a short QGP phase into the hadron resonance gas, through a mixed phase. The shadowing effects, implemented through the EPS09 parametrization, cancel out in the double ratio, as in the previous model. The result of the calculation, also shown in Fig. 3, is in fair agreement with the measured values, in particular for central collisions. The model uncertainties are dominated by the evaluation of the charmonium dissociation rates. The ALICE result is also compared to mid-rapidity ($|y| < 0.35$) PHENIX data [17] in Fig. 3. Remarkably, in spite of the very different $\sqrt{s_{\rm NN}}$ and $y_{\rm cms}$ values,

the observed patterns as a function of centrality are similar. It should also be noted that the PHENIX result can be qualitatively described in a hadronic dissociation scenario, as discussed in [38,42].

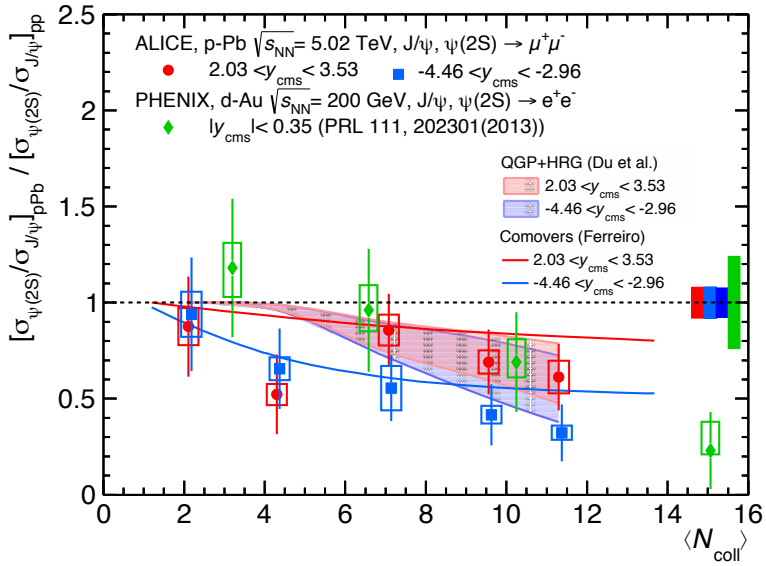

Fig. 3: Double ratio $[\sigma_{\psi(2S)}/\sigma_{J/\psi}]_{pPb}/[\sigma_{\psi(2S)}/\sigma_{J/\psi}]_{pp}$ for p-Pb and Pb-p collisions, shown as a function of $\langle N_{coll}\rangle$ (Pb-p points are slightly shifted in $\langle N_{coll}\rangle$ to improve visibility). The data are compared to PHENIX mid-rapidity results [17] and to the theoretical calculations of Ref. [38] and [42]. The boxes around unity correspond to the global systematic uncertainties at forward (red box) and backward (blue box) rapidities. The grey box is a global systematic uncertainty common to both p-Pb rapidity ranges, while the green box refers to the PHENIX results.

In Fig. 4 the nuclear modification factor for ψ(2S) mesons is shown as a function of centrality, separately for forward and backward rapidities. In both regions, a trend towards an increasing suppression can be seen when moving from peripheral to central collisions. The corresponding $Q_{pPb}^{J/\psi}$ values [24] are also shown. At forward-y there is an indication for a smaller $Q_{pPb}^{\psi(2S)}$ with respect to $Q_{pPb}^{J/\psi}$. The difference between the ψ(2S) and the J/ψ nuclear modification factors amounts, for central events, to 1.9σ, while, integrating over centrality, the corresponding quantity is 2.3σ. At backward-y the suppression patterns for the J/ψ and the ψ(2S) are different, with $Q_{pPb}^{J/\psi} \sim 1$ (or even slightly larger), and a strong suppression for the ψ(2S). In the most central collisions, the difference between the measured Q_{pPb} corresponds to 4.3σ, while, integrating over centrality, suppressions differ by 4.1σ. The results are compared to calculations including either only shadowing (EPS09 LO [38], EPS09 NLO [43]) or only coherent energy loss [44] and to models implementing final state interactions (co-movers [38], QGP+HRG [42]). While the J/ψ results are reproduced by shadowing/energy loss calculations, additional final state effects, as those discussed in the context of Fig. 3, are needed to describe the ψ(2S) results, in particular at backward rapidity.

Finally, the results are shown in Fig. 5 as a function of the pair crossing time τ_c in nuclear matter [9]. This quantity can be calculated as $\tau_c = \langle L\rangle/(\beta_z\gamma)$ where $\langle L\rangle$ is the average thickness of nuclear matter crossed by the pair, which was evaluated, for each centrality class, using the Glauber model [45], $\beta_z = \tanh y_{c\bar{c}}^{rest}$ is the velocity of the $c\bar{c}$ along the beam direction in the nucleus rest frame, $\gamma = E_{c\bar{c}}/m_{c\bar{c}}$ and $E_{c\bar{c}} = m_{T,c\bar{c}}\cosh y_{c\bar{c}}^{rest}$. The value $m_{c\bar{c}} = 3.4$ GeV/c^2 was chosen for the (average) mass of the evolving $c\bar{c}$ pair [9,46], while $m_{T,c\bar{c}}$ was calculated in each centrality bin starting from the measured J/ψ $\langle p_T\rangle$ values [24]. We use the J/ψ $\langle p_T\rangle$ as a proxy for the average p_T of the $c\bar{c}$ pair, as the $\psi(2S)$ statistics is too low to extract a corresponding $\langle p_T\rangle$ value. If we assume instead that $\langle p_T^{\psi(2S)}\rangle \sim 1.1\langle p_T^{J/\psi}\rangle$ as measured by LHCb in pp collisions at $\sqrt{s} = 7$ TeV [47,48], the τ_c values would decrease by $\sim 4\%$. Other sources of uncertainties on τ_c include the uncertainties on the measured J/ψ $\langle p_T\rangle$, which contribute less than 1%,

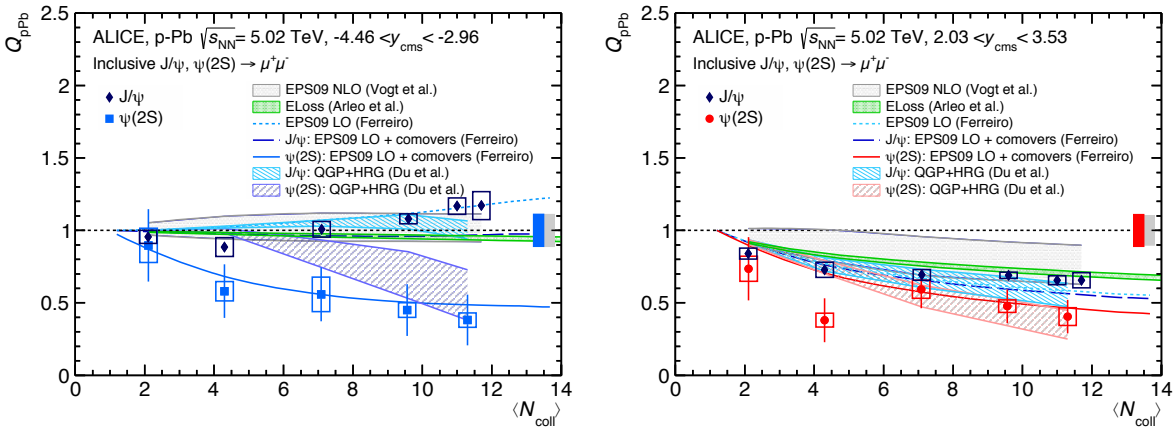

Fig. 4: J/ψ [24] and $\psi(2S)$ nuclear modification factors, $Q_{\rm pPb}$, shown as a function of $\langle N_{\rm coll} \rangle$ for the backward (left) and forward (right) rapidity regions and compared to theoretical models [38,42–44]. The boxes around unity correspond to the global $\psi(2S)$ systematic uncertainties at forward (red box) and backward (blue box) rapidities. The grey box is a global systematic uncertainty common to both J/ψ and $\psi(2S)$.

and those on $\langle L \rangle$, which are dominant and of the order of 10%. In Fig. 5 we show the double ratio as a function of $\tau_{\rm c}$ in the two rapidity regions. Different $\tau_{\rm c}$ intervals can also be selected by slicing the events in bins of $p_{\rm T}$ (see Ref. [33]), varying, in this way, the γ values of the $c\overline{c}$. The double ratio results, obtained in [33], are therefore also shown in Fig. 5 at their corresponding average $\tau_{\rm c}$ values. In the double ratio one effectively removes, as discussed above, initial state effects, so that Fig. 5 shows the $\tau_{\rm c}$ dependence of final state interactions on $\psi(2S)$ compared to J/ψ. The two sets of results, corresponding to a slicing of the events in centrality or in $p_{\rm T}$, are in good agreement. At backward-y, where the largest $\tau_{\rm c}$ values are reached, a clearly decreasing trend can be observed. The average resonance formation time $\tau_{\rm f}$ is, according to most theory estimates [9,18,19], larger by at least a factor ~ 2 than the accessible $\tau_{\rm c}$ range. On the other hand, the width of the $\tau_{\rm f}$ distribution is expected to be non-negligible [19], and it cannot be excluded that at least a fraction of the $c\overline{c}$ pairs hadronizes inside the nucleus. Therefore, the observed behaviour is likely due to a combination of final state effects which take place outside the nucleus, as e.g. interaction with a hadronic resonance gas, and dissociation effects on the fully formed resonance, due to nuclear matter, and taking place inside the nucleus. The relative importance of the two mechanisms is difficult to quantify in such a simple analysis and quantitative theoretical studies, also exploring alternative mechanisms, are needed. At forward rapidity, where $\tau_{\rm c}$ becomes smaller than $\tau_{\rm f}$ by about 2–3 orders of magnitude, the interaction with nuclear matter is not expected to play any significant role. The results of a similar analysis carried out on PHENIX mid-rapidity data [17] are also shown in Fig. 5. Within uncertainties, a scaling of the ALICE and PHENIX double ratio values with $\tau_{\rm c}$ is observed.

5 Conclusions

The centrality dependence of the $\psi(2S)$ production in p-Pb collisions at $\sqrt{s_{\rm NN}} = 5.02$ TeV was measured in five intervals, using the ZN energy as an estimator. The ratio $\mathrm{B.R.}_{\psi(2S)\to\mu^+\mu^-}\sigma_{\psi(2S)}/\mathrm{B.R.}_{J/\psi\to\mu^+\mu^-}\sigma_{J/\psi}$ is compatible with pp measurements in peripheral events, whereas a decrease is observed towards central events, showing that the $\psi(2S)$ state is suppressed with respect to the J/ψ. The results on the double ratio $[\sigma_{\psi(2S)}/\sigma_{J/\psi}]_{\rm pPb}/[\sigma_{\psi(2S)}/\sigma_{J/\psi}]_{\rm pp}$, as well as on the nuclear modification factors, show that effects such as shadowing or energy loss are enough to explain the J/ψ behaviour, while additional mechanisms are needed to describe the $\psi(2S)$ suppression. Theoretical models that include final state interactions are able to reproduce the data. A study of the double ratio as a function of the crossing time $\tau_{\rm c}$ shows that at forward-y the $\tau_{\rm c}$ values are much shorter than the resonance formation time $\tau_{\rm f}$, excluding any significant role of final state interactions with nuclear matter. Effects occurring at later times, such as the break-up by co-movers in the hadronic gas, are suitable candidates for an explanation of the observed

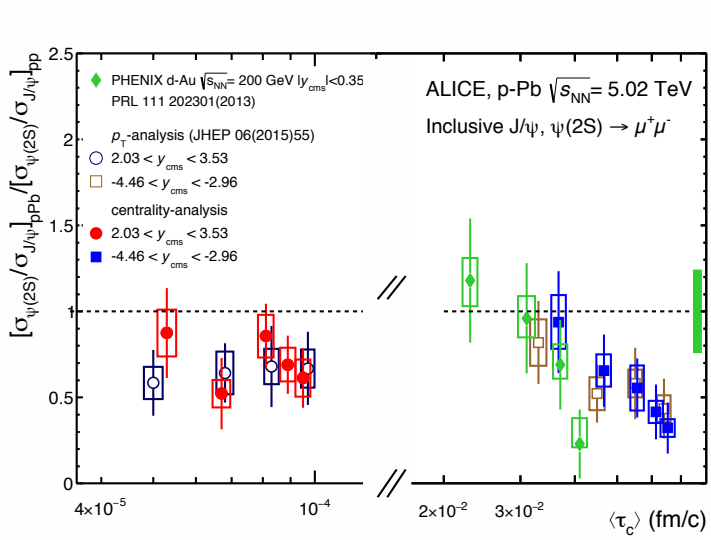

Fig. 5: Double ratio $[\sigma_{\psi(2S)}/\sigma_{J/\psi}]_{pPb}/[\sigma_{\psi(2S)}/\sigma_{J/\psi}]_{pp}$ shown as a function of τ_c for the backward and forward rapidity regions. For each y-range, the two sets of points were obtained from the centrality analysis and from the p_T-dependent analysis of Ref. [20]. Statistical uncertainties are shown as lines, while the total systematic uncertainties are shown as boxes around the points. The results of a corresponding analysis carried out on the PHENIX mid-rapidity data [17] is also shown. The box around unity represents the PHENIX global systematic uncertainty.

$\psi(2S)$ suppression. At backward-y the τ_c values, although significantly larger, are still smaller than τ_f. However, the observed scaling of the double ratios with τ_c may be suggestive of an effect at least partly related to a dissociation of the fully-formed resonance in nuclear matter.

Acknowledgements

The ALICE Collaboration would like to thank all its engineers and technicians for their invaluable contributions to the construction of the experiment and the CERN accelerator teams for the outstanding performance of the LHC complex. The ALICE Collaboration gratefully acknowledges the resources and support provided by all Grid centres and the Worldwide LHC Computing Grid (WLCG) collaboration. The ALICE Collaboration acknowledges the following funding agencies for their support in building and running the ALICE detector: State Committee of Science, World Federation of Scientists (WFS) and Swiss Fonds Kidagan, Armenia; Conselho Nacional de Desenvolvimento Científico e Tecnológico (CNPq), Financiadora de Estudos e Projetos (FINEP), Fundação de Amparo à Pesquisa do Estado de São Paulo (FAPESP); National Natural Science Foundation of China (NSFC), the Chinese Ministry of Education (CMOE) and the Ministry of Science and Technology of China (MSTC); Ministry of Education and Youth of the Czech Republic; Danish Natural Science Research Council, the Carlsberg Foundation and the Danish National Research Foundation; The European Research Council under the European Community's Seventh Framework Programme; Helsinki Institute of Physics and the Academy of Finland; French CNRS-IN2P3, the 'Region Pays de Loire', 'Region Alsace', 'Region Auvergne' and CEA, France; German Bundesministerium fur Bildung, Wissenschaft, Forschung und Technologie (BMBF) and the Helmholtz Association; General Secretariat for Research and Technology, Ministry of Development, Greece; National Research, Development and Innovation Office (NKFIH), Hungary; Department of Atomic Energy and Department of Science and Technology of the Government of India; Istituto Nazionale di Fisica Nucleare (INFN) and Centro Fermi - Museo Storico della Fisica e Centro Studi e Ricerche "Enrico Fermi", Italy; Japan Society for the Promotion of Science (JSPS) KAKENHI and MEXT, Japan; Joint Institute for Nuclear Research, Dubna; National Research Foun-

dation of Korea (NRF); Consejo Nacional de Cienca y Tecnologia (CONACYT), Direccion General de Asuntos del Personal Academico(DGAPA), México, Amerique Latine Formation academique - European Commission (ALFA-EC) and the EPLANET Program (European Particle Physics Latin American Network); Stichting voor Fundamenteel Onderzoek der Materie (FOM) and the Nederlandse Organisatie voor Wetenschappelijk Onderzoek (NWO), Netherlands; Research Council of Norway (NFR); National Science Centre, Poland; Ministry of National Education/Institute for Atomic Physics and National Council of Scientific Research in Higher Education (CNCSI-UEFISCDI), Romania; Ministry of Education and Science of Russian Federation, Russian Academy of Sciences, Russian Federal Agency of Atomic Energy, Russian Federal Agency for Science and Innovations and The Russian Foundation for Basic Research; Ministry of Education of Slovakia; Department of Science and Technology, South Africa; Centro de Investigaciones Energeticas, Medioambientales y Tecnologicas (CIEMAT), E-Infrastructure shared between Europe and Latin America (EELA), Ministerio de Economía y Competitividad (MINECO) of Spain, Xunta de Galicia (Consellería de Educación), Centro de Aplicaciones Tecnolgicas y Desarrollo Nuclear (CEADEN), Cubaenergía, Cuba, and IAEA (International Atomic Energy Agency); Swedish Research Council (VR) and Knut & Alice Wallenberg Foundation (KAW); Ukraine Ministry of Education and Science; United Kingdom Science and Technology Facilities Council (STFC); The United States Department of Energy, the United States National Science Foundation, the State of Texas, and the State of Ohio; Ministry of Science, Education and Sports of Croatia and Unity through Knowledge Fund, Croatia; Council of Scientific and Industrial Research (CSIR), New Delhi, India; Pontificia Universidad Católica del Perú.

References

[1] N. Brambilla *et al.*, "Heavy quarkonium: progress, puzzles, and opportunities," *Eur. Phys. J.* **C71** (2011) 1534, arXiv:1010.5827 [hep-ph].

[2] A. Andronic *et al.*, "Heavy-flavour and quarkonium production in the LHC era: from proton-proton to heavy-ion collisions," arXiv:1506.03981 [nucl-ex].

[3] K. Eskola, H. Paukkunen, and C. Salgado, "EPS09: A new generation of NLO and LO nuclear parton distribution functions," *JHEP* **0904** (2009) 065, arXiv:0902.4154 [hep-ph].

[4] D. de Florian, R. Sassot, P. Zurita, and M. Stratmann, "Global analysis of nuclear parton distributions," *Phys. Rev.* **D85** (2012) 074028, arXiv:1112.6324 [hep-ph].

[5] M. Hirai, S. Kumano, and T. H. Nagai, "Determination of nuclear parton distribution functions and their uncertainties in next-to-leading order," *Phys. Rev.* **C76** (2007) 065207, arXiv:0709.3038 [hep-ph].

[6] F. Arleo and S. Peigne, "J/ψ suppression in p-A collisions from parton energy loss in cold QCD matter," *Phys.Rev.Lett.* **109** (2012) 122301, arXiv:1204.4609 [hep-ph].

[7] R. Vogt, "Are the J/ψ and χ_c A dependencies the same?," *Nucl.Phys.* **A700** (2002) 539–554, arXiv:hep-ph/0107045 [hep-ph].

[8] B. Kopeliovich and B. Zakharov, "Quantum effects and color transparency in charmonium photoproduction on nuclei," *Phys.Rev.* **D44** (1991) 3466–3472.

[9] D. McGlinchey, A. Frawley, and R. Vogt, "Impact parameter dependence of the nuclear modification of J/ψ production in d+Au collisions at $\sqrt{s_{\rm NN}} = 200$ GeV," *Phys.Rev.* **C87** no. 5, (2013) 054910, arXiv:1208.2667 [nucl-th].

[10] H. Satz, "Colour deconfinement and quarkonium binding," *J. Phys.* **G32** (2006) R25, arXiv:hep-ph/0512217 [hep-ph].

[11] R. Vogt, "The x(F) dependence of ψ and Drell-Yan production," *Phys.Rev.* **C61** (2000) 035203, arXiv:hep-ph/9907317 [hep-ph].

[12] **NuSea** Collaboration, M. Leitch *et al.*, "Measurement of J /ψ and ψ' suppression in p-A collisions

at 800-GeV/c," *Phys.Rev.Lett.* **84** (2000) 3256–3260, arXiv:nucl-ex/9909007 [nucl-ex].

[13] **HERA-B** Collaboration, I. Abt *et al.*, "A Measurement of the ψ' to J/ψ production ratio in 920-GeV proton-nucleus interactions," *Eur.Phys.J.* **C49** (2007) 545–558, arXiv:hep-ex/0607046 [hep-ex].

[14] **NA50** Collaboration, B. Alessandro *et al.*, "J/ψ and ψ' production and their normal nuclear absorption in proton-nucleus collisions at 400-GeV," *Eur.Phys.J.* **C48** (2006) 329, arXiv:nucl-ex/0612012 [nucl-ex].

[15] **NA50** Collaboration, B. Alessandro *et al.*, "Charmonium production and nuclear absorption in p-A interactions at 450-GeV," *Eur.Phys.J.* **C33** (2004) 31–40.

[16] **NA60** Collaboration, R. Arnaldi *et al.*, "J/ψ production in proton-nucleus collisions at 158 and 400 GeV," *Phys.Lett.* **B706** (2012) 263–267, arXiv:1004.5523 [nucl-ex].

[17] **PHENIX** Collaboration, A. Adare *et al.*, "Nuclear Modification of ψ', χ_c, and J/ψ production in d+Au collisions at $\sqrt{s_{NN}}$=200 GeV," *Phys.Rev.Lett.* **111** no. 20, (2013) 202301, arXiv:1305.5516 [nucl-ex].

[18] J. Hufner, Yu. P. Ivanov, B. Z. Kopeliovich, and A. V. Tarasov, "Photoproduction of charmonia and total charmonium proton cross-sections," *Phys. Rev.* **D62** (2000) 094022, arXiv:hep-ph/0007111 [hep-ph].

[19] D. Kharzeev and R. L. Thews, "Quarkonium formation time in a model independent approach," *Phys. Rev.* **C60** (1999) 041901, arXiv:nucl-th/9907021 [nucl-th].

[20] **ALICE** Collaboration, B. Abelev *et al.*, "Suppression of ψ(2S) production in p-Pb collisions at $\sqrt{s_{NN}}$ = 5.02 TeV," *JHEP* **1412** (2014) 073, arXiv:1405.3796 [nucl-ex].

[21] **ALICE** Collaboration, B. Abelev *et al.*, "J/ψ production and nuclear effects in p-Pb collisions at $\sqrt{S_{NN}}$ = 5.02 TeV," *JHEP* **1402** (2014) 073, arXiv:1308.6726 [nucl-ex].

[22] **LHCb** Collaboration, R. Aaij *et al.*, "Study of $\psi(2S)$ production and cold nuclear matter effects in pPb collisions at $\sqrt{s_{NN}} = 5$ TeV," arXiv:1601.07878 [nucl-ex].

[23] **LHCb** Collaboration, R. Aaij *et al.*, "Study of J/ψ production and cold nuclear matter effects in *pPb* collisions at $\sqrt{s_{NN}} = 5$ TeV," *JHEP* **02** (2014) 072, arXiv:1308.6729 [nucl-ex].

[24] **ALICE** Collaboration, J. Adam *et al.*, "Centrality dependence of inclusive J/ψ production in p-Pb collisions at $\sqrt{s\_\mathrm{NN}}$ = 5.02 TeV," arXiv:1506.08808 [nucl-ex].

[25] **ALICE** Collaboration, K. Aamodt *et al.*, "Rapidity and transverse momentum dependence of inclusive J/ψ production in *pp* collisions at $\sqrt{s} = 7$ TeV," *Phys.Lett.* **B704** (2011) 442–455, arXiv:1105.0380 [hep-ex].

[26] **ALICE** Collaboration, K. Aamodt *et al.*, "The ALICE experiment at the CERN LHC," *JINST* **3** (2008) S08002.

[27] **ALICE** Collaboration, K. Aamodt *et al.*, "Alignment of the ALICE Inner Tracking System with cosmic-ray tracks," *JINST* **5** (2010) P03003, arXiv:1001.0502 [physics.ins-det].

[28] **ALICE** Collaboration, E. Abbas *et al.*, "Performance of the ALICE VZERO system," *JINST* **8** (2013) P10016, arXiv:1306.3130 [nucl-ex].

[29] **ALICE** Collaboration, B. Abelev *et al.*, "Measurement of the cross section for electromagnetic dissociation with neutron emission in Pb-Pb collisions at $\sqrt{s_{NN}}$ = 2.76 TeV," *Phys.Rev.Lett.* **109** (2012) 252302, arXiv:1203.2436 [nucl-ex].

[30] **ALICE** Collaboration, J. Adam *et al.*, "Centrality dependence of particle production in p-Pb collisions at $\sqrt{s_{\mathrm{NN}}}$= 5.02 TeV," *Phys.Rev.* **C91** no. 6, (2015) 064905, arXiv:1412.6828 [nucl-ex].

[31] **ALICE** Collaboration, B. B. Abelev *et al.*, "Performance of the ALICE Experiment at the CERN LHC," *Int. J. Mod. Phys.* **A29** (2014) 1430044, arXiv:1402.4476 [nucl-ex].

[32] **ALICE** Collaboration, B. Abelev *et al.*, "Measurement of visible cross sections in proton-lead

collisions at $\sqrt{s_{\rm NN}}$ = 5.02 TeV in van der Meer scans with the ALICE detector," *JINST* **9** no. 11, (2014) P11003, arXiv:1405.1849 [nucl-ex].

[33] **ALICE** Collaboration, J. Adam *et al.*, "Rapidity and transverse-momentum dependence of the inclusive J/ψ nuclear modification factor in p-Pb collisions at $\sqrt{s_{N\,N}} = 5.02$ TeV," *JHEP* **1506** (2015) 055, arXiv:1503.07179 [nucl-ex].

[34] F. Sikler, "Centrality control of hadron nucleus interactions by detection of slow nucleons," arXiv:hep-ph/0304065 [hep-ph].

[35] **E910** Collaboration, I. Chemakin *et al.*, "Measuring centrality with slow protons in proton nucleus collisions at the AGS," *Phys. Rev.* **C60** (1999) 024902, arXiv:nucl-ex/9902003 [nucl-ex].

[36] **ALICE** Collaboration, J. Adam *et al.*, "Quarkonium signal extraction in ALICE," *ALICE-PUBLIC-2015-006* (2015) .

[37] **ALICE** Collaboration, B. Abelev *et al.*, "Measurement of quarkonium production at forward rapidity in pp collisions at $\sqrt{s} = 7$ TeV," *Eur. Phys. J.* **C74** no. 8, (2014) 2974, arXiv:1403.3648 [nucl-ex].

[38] E. G. Ferreiro, "Excited charmonium suppression in proton-nucleus collisions as a consequence of comovers," *Phys. Lett.* **B749** (2015) 98–103, arXiv:1411.0549 [hep-ph].

[39] N. Armesto and A. Capella, "A Quantitative reanalysis of J/ψ suppression in nuclear collisions," *Phys. Lett.* **B430** (1998) 23–31, arXiv:hep-ph/9705275 [hep-ph].

[40] **ALICE** Collaboration, B. Abelev *et al.*, "Pseudorapidity density of charged particles in p + Pb collisions at $\sqrt{s_{NN}} = 5.02$ TeV," *Phys. Rev. Lett.* **110** no. 3, (2013) 032301, arXiv:1210.3615 [nucl-ex].

[41] X. Zhao and R. Rapp, "Charmonium in medium: from correlators to experiment," *Phys. Rev.* **C82** (2010) 064905, arXiv:1008.5328 [hep-ph].

[42] X. Du and R. Rapp, "Sequential regeneration of charmonia in heavy-ion collisions," arXiv:1504.00670 [hep-ph].

[43] R. Vogt, "Shadowing effects on J/ψ and Υ production at the LHC," arXiv:1507.04418 [hep-ph].

[44] F. Arleo, R. Kolevatov, S. Peignè, and M. Rustamova, "Centrality and $p_{\rm T}$ dependence of J/ψ suppression in proton-nucleus collisions from parton energy loss," *JHEP* **1305** (2013) 155, arXiv:1304.0901 [hep-ph].

[45] M. L. Miller, K. Reygers, S. J. Sanders, and P. Steinberg, "Glauber modeling in high energy nuclear collisions," *Ann. Rev. Nucl. Part. Sci.* **57** (2007) 205–243, arXiv:nucl-ex/0701025 [nucl-ex].

[46] F. Arleo, P. Gossiaux, T. Gousset, and J. Aichelin, "Charmonium suppression in p-A collisions," *Phys.Rev.* **C61** (2000) 054906, arXiv:hep-ph/9907286 [hep-ph].

[47] **LHCb** Collaboration, R. Aaij *et al.*, "Measurement of $\psi(2S)$ meson production in pp collisions at $\sqrt{s}$=7 TeV," *Eur. Phys. J.* **C72** (2012) 2100, arXiv:1204.1258 [hep-ex].

[48] **LHCb** Collaboration, R. Aaij *et al.*, "Measurement of J/ψ polarization in pp collisions at $\sqrt{s} = 7$ TeV," *Eur. Phys. J.* **C73** no. 11, (2013) 2631, arXiv:1307.6379 [hep-ex].

A The ALICE Collaboration

J. Adam[39], D. Adamová[84], M.M. Aggarwal[88], G. Aglieri Rinella[35], M. Agnello[110], N. Agrawal[47], Z. Ahammed[133], S. Ahmad[18], S.U. Ahn[68], S. Aiola[137], A. Akindinov[54], S.N. Alam[133], D.S.D. Albuquerque[121], D. Aleksandrov[80], B. Alessandro[110], D. Alexandre[101], R. Alfaro Molina[63], A. Alici[12,104], A. Alkin[3], J.R.M. Almaraz[119], J. Alme[22,37], T. Alt[42], S. Altinpinar[22], I. Altsybeev[132], C. Alves Garcia Prado[120], C. Andrei[78], A. Andronic[97], V. Anguelov[93], T. Antičić[98], F. Antinori[107], P. Antonioli[104], L. Aphecetche[113], H. Appelshäuser[60], S. Arcelli[27], R. Arnaldi[110], O.W. Arnold[36,94], I.C. Arsene[21], M. Arslandok[60], B. Audurier[113], A. Augustinus[35], R. Averbeck[97], M.D. Azmi[18], A. Badalà[106], Y.W. Baek[67], S. Bagnasco[110], R. Bailhache[60], R. Bala[91], S. Balasubramanian[137], A. Baldisseri[15], R.C. Baral[57], A.M. Barbano[26], R. Barbera[28], F. Barile[32], G.G. Barnaföldi[136], L.S. Barnby[35,101], V. Barret[70], P. Bartalini[7], K. Barth[35], J. Bartke[117], E. Bartsch[60], M. Basile[27], N. Bastid[70], S. Basu[133], B. Bathen[61], G. Batigne[113], A. Batista Camejo[70], B. Batyunya[66], P.C. Batzing[21], I.G. Bearden[81], H. Beck[60,93], C. Bedda[110], N.K. Behera[48,50], I. Belikov[64], F. Bellini[27], H. Bello Martinez[2], R. Bellwied[122], R. Belmont[135], E. Belmont-Moreno[63], V. Belyaev[75], G. Bencedi[136], S. Beole[26], I. Berceanu[78], A. Bercuci[78], Y. Berdnikov[86], D. Berenyi[136], R.A. Bertens[53], D. Berzano[35], L. Betev[35], A. Bhasin[91], I.R. Bhat[91], A.K. Bhati[88], B. Bhattacharjee[44], J. Bhom[117,128], L. Bianchi[122], N. Bianchi[72], C. Bianchin[135], J. Bielčík[39], J. Bielčíková[84], A. Bilandzic[36,81,94], G. Biro[136], R. Biswas[4], S. Biswas[4,79], S. Bjelogrlic[53], J.T. Blair[118], D. Blau[80], C. Blume[60], F. Bock[74,93], A. Bogdanov[75], H. Bøggild[81], L. Boldizsár[136], M. Bombara[40], J. Book[60], H. Borel[15], A. Borissov[96], M. Borri[83,124], F. Bossú[65], E. Botta[26], C. Bourjau[81], P. Braun-Munzinger[97], M. Bregant[120], T. Breitner[59], T.A. Broker[60], T.A. Browning[95], M. Broz[39], E.J. Brucken[45], E. Bruna[110], G.E. Bruno[32], D. Budnikov[99], H. Buesching[60], S. Bufalino[26,35], P. Buncic[35], O. Busch[128], Z. Buthelezi[65], J.B. Butt[16], J.T. Buxton[19], J. Cabala[115], D. Caffarri[35], X. Cai[7], H. Caines[137], L. Calero Diaz[72], A. Caliva[53], E. Calvo Villar[102], P. Camerini[25], F. Carena[35], W. Carena[35], F. Carnesecchi[27], J. Castillo Castellanos[15], A.J. Castro[125], E.A.R. Casula[24], C. Ceballos Sanchez[9], J. Cepila[39], P. Cerello[110], J. Cerkala[115], B. Chang[123], S. Chapeland[35], M. Chartier[124], J.L. Charvet[15], S. Chattopadhyay[133], S. Chattopadhyay[100], A. Chauvin[36,94], V. Chelnokov[3], M. Cherney[87], C. Cheshkov[130], B. Cheynis[130], V. Chibante Barroso[35], D.D. Chinellato[121], S. Cho[50], P. Chochula[35], K. Choi[96], M. Chojnacki[81], S. Choudhury[133], P. Christakoglou[82], C.H. Christensen[81], P. Christiansen[33], T. Chujo[128], S.U. Chung[96], C. Cicalo[105], L. Cifarelli[12,27], F. Cindolo[104], J. Cleymans[90], F. Colamaria[32], D. Colella[35,55], A. Collu[74], M. Colocci[27], G. Conesa Balbastre[71], Z. Conesa del Valle[51], M.E. Connors[II,137], J.G. Contreras[39], T.M. Cormier[85], Y. Corrales Morales[110], I. Cortés Maldonado[2], P. Cortese[31], M.R. Cosentino[120], F. Costa[35], P. Crochet[70], R. Cruz Albino[11], E. Cuautle[62], L. Cunqueiro[35,61], T. Dahms[36,94], A. Dainese[107], M.C. Danisch[93], A. Danu[58], D. Das[100], I. Das[100], S. Das[4], A. Dash[79], S. Dash[47], S. De[120], A. De Caro[12,30], G. de Cataldo[103], C. de Conti[120], J. de Cuveland[42], A. De Falco[24], D. De Gruttola[12,30], N. De Marco[110], S. De Pasquale[30], A. Deisting[93,97], A. Deloff[77], E. Dénes[I,136], C. Deplano[82], P. Dhankher[47], D. Di Bari[32], A. Di Mauro[35], P. Di Nezza[72], M.A. Diaz Corchero[10], T. Dietel[90], P. Dillenseger[60], R. Divià[35], Ø. Djuvsland[22], A. Dobrin[58,82], D. Domenicis Gimenez[120], B. Dönigus[60], O. Dordic[21], T. Drozhzhova[60], A.K. Dubey[133], A. Dubla[53], L. Ducroux[130], P. Dupieux[70], R.J. Ehlers[137], D. Elia[103], E. Endress[102], H. Engel[59], E. Epple[36,94,137], B. Erazmus[113], I. Erdemir[60], F. Erhardt[129], B. Espagnon[51], M. Estienne[113], S. Esumi[128], J. Eum[96], D. Evans[101], S. Evdokimov[111], G. Eyyubova[39], L. Fabbietti[36,94], D. Fabris[107], J. Faivre[71], A. Fantoni[72], M. Fasel[74], L. Feldkamp[61], A. Feliciello[110], G. Feofilov[132], J. Ferencei[84], A. Fernández Téllez[2], E.G. Ferreiro[17], A. Ferretti[26], A. Festanti[29], V.J.G. Feuillard[15,70], J. Figiel[117], M.A.S. Figueredo[120,124], S. Filchagin[99], D. Finogeev[52], F.M. Fionda[24], E.M. Fiore[32], M.G. Fleck[93], M. Floris[35], S. Foertsch[65], P. Foka[97], S. Fokin[80], E. Fragiacomo[109], A. Francescon[29,35], U. Frankenfeld[97], G.G. Fronze[26], U. Fuchs[35], C. Furget[71], A. Furs[52], M. Fusco Girard[30], J.J. Gaardhøje[81], M. Gagliardi[26], A.M. Gago[102], M. Gallio[26], D.R. Gangadharan[74], P. Ganoti[89], C. Gao[7], C. Garabatos[97], E. Garcia-Solis[13], C. Gargiulo[35], P. Gasik[36,94], E.F. Gauger[118], M. Germain[113], M. Gheata[35,58], P. Ghosh[133], S.K. Ghosh[4], P. Gianotti[72], P. Giubellino[35,110], P. Giubilato[29], E. Gladysz-Dziadus[117], P. Glässel[93], D.M. Goméz Coral[63], A. Gomez Ramirez[59], A.S. Gonzalez[35], V. Gonzalez[10], P. González-Zamora[10], S. Gorbunov[42], L. Görlich[117], S. Gotovac[116], V. Grabski[63], O.A. Grachov[137], L.K. Graczykowski[134],

K.L. Graham[101], A. Grelli[53], A. Grigoras[35], C. Grigoras[35], V. Grigoriev[75], A. Grigoryan[1], S. Grigoryan[66], B. Grinyov[3], N. Grion[109], J.M. Gronefeld[97], J.F. Grosse-Oetringhaus[35], R. Grosso[97], F. Guber[52], R. Guernane[71], B. Guerzoni[27], K. Gulbrandsen[81], T. Gunji[127], A. Gupta[91], R. Gupta[91], R. Haake[35], Ø. Haaland[22], C. Hadjidakis[51], M. Haiduc[58], H. Hamagaki[127], G. Hamar[136], J.C. Hamon[64], J.W. Harris[137], A. Harton[13], D. Hatzifotiadou[104], S. Hayashi[127], S.T. Heckel[60], E. Hellbär[60], H. Helstrup[37], A. Herghelegiu[78], G. Herrera Corral[11], B.A. Hess[34], K.F. Hetland[37], H. Hillemanns[35], B. Hippolyte[64], D. Horak[39], R. Hosokawa[128], P. Hristov[35], T.J. Humanic[19], N. Hussain[44], T. Hussain[18], D. Hutter[42], D.S. Hwang[20], R. Ilkaev[99], M. Inaba[128], E. Incani[24], M. Ippolitov[75,80], M. Irfan[18], M. Ivanov[97], V. Ivanov[86], V. Izucheev[111], N. Jacazio[27], P.M. Jacobs[74], M.B. Jadhav[47], S. Jadlovska[115], J. Jadlovsky[55,115], C. Jahnke[120], M.J. Jakubowska[134], H.J. Jang[68], M.A. Janik[134], P.H.S.Y. Jayarathna[122], C. Jena[29], S. Jena[122], R.T. Jimenez Bustamante[97], P.G. Jones[101], A. Jusko[101], P. Kalinak[55], A. Kalweit[35], J. Kamin[60], J.H. Kang[138], V. Kaplin[75], S. Kar[133], A. Karasu Uysal[69], O. Karavichev[52], T. Karavicheva[52], L. Karayan[93,97], E. Karpechev[52], U. Kebschull[59], R. Keidel[139], D.L.D. Keijdener[53], M. Keil[35], M. Mohisin Khan[III,18], P. Khan[100], S.A. Khan[133], A. Khanzadeev[86], Y. Kharlov[111], B. Kileng[37], D.W. Kim[43], D.J. Kim[123], D. Kim[138], H. Kim[138], J.S. Kim[43], M. Kim[138], S. Kim[20], T. Kim[138], S. Kirsch[42], I. Kisel[42], S. Kiselev[54], A. Kisiel[134], G. Kiss[136], J.L. Klay[6], C. Klein[60], J. Klein[35], C. Klein-Bösing[61], S. Klewin[93], A. Kluge[35], M.L. Knichel[93], A.G. Knospe[118,122], C. Kobdaj[114], M. Kofarago[35], T. Kollegger[97], A. Kolojvari[132], V. Kondratiev[132], N. Kondratyeva[75], E. Kondratyuk[111], A. Konevskikh[52], M. Kopcik[115], P. Kostarakis[89], M. Kour[91], C. Kouzinopoulos[35], O. Kovalenko[77], V. Kovalenko[132], M. Kowalski[117], G. Koyithatta Meethaleveedu[47], I. Králik[55], A. Kravčáková[40], M. Krivda[55,101], F. Krizek[84], E. Kryshen[35,86], M. Krzewicki[42], A.M. Kubera[19], V. Kučera[84], C. Kuhn[64], P.G. Kuijer[82], A. Kumar[91], J. Kumar[47], L. Kumar[88], S. Kumar[47], P. Kurashvili[77], A. Kurepin[52], A.B. Kurepin[52], A. Kuryakin[99], M.J. Kweon[50], Y. Kwon[138], S.L. La Pointe[110], P. La Rocca[28], P. Ladron de Guevara[11], C. Lagana Fernandes[120], I. Lakomov[35], R. Langoy[41], K. Lapidus[36,94], C. Lara[59], A. Lardeux[15], A. Lattuca[26], E. Laudi[35], R. Lea[25], L. Leardini[93], G.R. Lee[101], S. Lee[138], F. Lehas[82], S. Lehner[112], R.C. Lemmon[83], V. Lenti[103], E. Leogrande[53], I. León Monzón[119], H. León Vargas[63], M. Leoncino[26], P. Lévai[136], S. Li[7,70], X. Li[14], J. Lien[41], R. Lietava[101], S. Lindal[21], V. Lindenstruth[42], C. Lippmann[97], M.A. Lisa[19], H.M. Ljunggren[33], D.F. Lodato[53], P.I. Loenne[22], V. Loginov[75], C. Loizides[74], X. Lopez[70], E. López Torres[9], A. Lowe[136], P. Luettig[60], M. Lunardon[29], G. Luparello[25], T.H. Lutz[137], A. Maevskaya[52], M. Mager[35], S. Mahajan[91], S.M. Mahmood[21], A. Maire[64], R.D. Majka[137], M. Malaev[86], I. Maldonado Cervantes[62], L. Malinina[IV,66], D. Mal'Kevich[54], P. Malzacher[97], A. Mamonov[99], V. Manko[80], F. Manso[70], V. Manzari[35,103], M. Marchisone[26,65,126], J. Mareš[56], G.V. Margagliotti[25], A. Margotti[104], J. Margutti[53], A. Marín[97], C. Markert[118], M. Marquard[60], N.A. Martin[97], J. Martin Blanco[113], P. Martinengo[35], M.I. Martínez[2], G. Martínez García[113], M. Martinez Pedreira[35], A. Mas[120], S. Masciocchi[97], M. Masera[26], A. Masoni[105], A. Mastroserio[32], A. Matyja[117], C. Mayer[117], J. Mazer[125], M.A. Mazzoni[108], D. Mcdonald[122], F. Meddi[23], Y. Melikyan[75], A. Menchaca-Rocha[63], E. Meninno[30], J. Mercado Pérez[93], M. Meres[38], Y. Miake[128], M.M. Mieskolainen[45], K. Mikhaylov[54,66], L. Milano[35,74], J. Milosevic[21], A. Mischke[53], A.N. Mishra[48], D. Miśkowiec[97], J. Mitra[133], C.M. Mitu[58], N. Mohammadi[53], B. Mohanty[79], L. Molnar[64], L. Montaño Zetina[11], E. Montes[10], D.A. Moreira De Godoy[61], L.A.P. Moreno[2], S. Moretto[29], A. Morreale[113], A. Morsch[35], V. Muccifora[72], E. Mudnic[116], D. Mühlheim[61], S. Muhuri[133], M. Mukherjee[133], J.D. Mulligan[137], M.G. Munhoz[120], R.H. Munzer[36,60,94], H. Murakami[127], S. Murray[65], L. Musa[35], J. Musinsky[55], B. Naik[47], R. Nair[77], B.K. Nandi[47], R. Nania[104], E. Nappi[103], M.U. Naru[16], H. Natal da Luz[120], C. Nattrass[125], S.R. Navarro[2], K. Nayak[79], R. Nayak[47], T.K. Nayak[133], S. Nazarenko[99], A. Nedosekin[54], L. Nellen[62], F. Ng[122], M. Nicassio[97], M. Niculescu[58], J. Niedziela[35], B.S. Nielsen[81], S. Nikolaev[80], S. Nikulin[80], V. Nikulin[86], F. Noferini[12,104], P. Nomokonov[66], G. Nooren[53], J.C.C. Noris[2], J. Norman[124], A. Nyanin[80], J. Nystrand[22], H. Oeschler[93], S. Oh[137], S.K. Oh[67], A. Ohlson[35], A. Okatan[69], T. Okubo[46], L. Olah[136], J. Oleniacz[134], A.C. Oliveira Da Silva[120], M.H. Oliver[137], J. Onderwaater[97], C. Oppedisano[110], R. Orava[45], M. Oravec[115], A. Ortiz Velasquez[62], A. Oskarsson[33], J. Otwinowski[117], K. Oyama[76,93], M. Ozdemir[60], Y. Pachmayer[93], D. Pagano[131], P. Pagano[30], G. Paić[62], S.K. Pal[133], J. Pan[135], A.K. Pandey[47], V. Papikyan[1], G.S. Pappalardo[106], P. Pareek[48], W.J. Park[97], S. Parmar[88], A. Passfeld[61], V. Paticchio[103], R.N. Patra[133], B. Paul[100,110], H. Pei[7], T. Peitzmann[53], H. Pereira Da Costa[15], D. Peresunko[75,80], E. Perez Lezama[60], V. Peskov[60], Y. Pestov[5], V. Petráček[39],

V. Petrov[111], M. Petrovici[78], C. Petta[28], S. Piano[109], M. Pikna[38], P. Pillot[113], L.O.D.L. Pimentel[81], O. Pinazza[35,104], L. Pinsky[122], D.B. Piyarathna[122], M. Płoskoń[74], M. Planinic[129], J. Pluta[134], S. Pochybova[136], P.L.M. Podesta-Lerma[119], M.G. Poghosyan[85,87], B. Polichtchouk[111], N. Poljak[129], W. Poonsawat[114], A. Pop[78], H. Poppenborg[61], S. Porteboeuf-Houssais[70], J. Porter[74], J. Pospisil[84], S.K. Prasad[4], R. Preghenella[35,104], F. Prino[110], C.A. Pruneau[135], I. Pshenichnov[52], M. Puccio[26], G. Puddu[24], P. Pujahari[135], V. Punin[99], J. Putschke[135], H. Qvigstad[21], A. Rachevski[109], S. Raha[4], S. Rajput[91], J. Rak[123], A. Rakotozafindrabe[15], L. Ramello[31], F. Rami[64], R. Raniwala[92], S. Raniwala[92], S.S. Räsänen[45], B.T. Rascanu[60], D. Rathee[88], K.F. Read[85,125], K. Redlich[77], R.J. Reed[135], A. Rehman[22], P. Reichelt[60], F. Reidt[35,93], X. Ren[7], R. Renfordt[60], A.R. Reolon[72], A. Reshetin[52], K. Reygers[93], V. Riabov[86], R.A. Ricci[73], T. Richert[33], M. Richter[21], P. Riedler[35], W. Riegler[35], F. Riggi[28], C. Ristea[58], E. Rocco[53], M. Rodríguez Cahuantzi[2,11], A. Rodriguez Manso[82], K. Røed[21], E. Rogochaya[66], D. Rohr[42], D. Röhrich[22], F. Ronchetti[35,72], L. Ronflette[113], P. Rosnet[70], A. Rossi[29,35], F. Roukoutakis[89], A. Roy[48], C. Roy[64], P. Roy[100], A.J. Rubio Montero[10], R. Rui[25], R. Russo[26], B.D. Ruzza[107], E. Ryabinkin[80], Y. Ryabov[86], A. Rybicki[117], S. Saarinen[45], S. Sadhu[133], S. Sadovsky[111], K. Šafařík[35], B. Sahlmuller[60], P. Sahoo[48], R. Sahoo[48], S. Sahoo[57], P.K. Sahu[57], J. Saini[133], S. Sakai[72], M.A. Saleh[135], J. Salzwedel[19], S. Sambyal[91], V. Samsonov[86], L. Šándor[55], A. Sandoval[63], M. Sano[128], D. Sarkar[133], N. Sarkar[133], P. Sarma[44], E. Scapparone[104], F. Scarlassara[29], C. Schiaua[78], R. Schicker[93], C. Schmidt[97], H.R. Schmidt[34], M. Schmidt[34], S. Schuchmann[60], J. Schukraft[35], M. Schulc[39], Y. Schutz[35,113], K. Schwarz[97], K. Schweda[97], G. Scioli[27], E. Scomparin[110], R. Scott[125], M. Šefčík[40], J.E. Seger[87], Y. Sekiguchi[127], D. Sekihata[46], I. Selyuzhenkov[97], K. Senosi[65], S. Senyukov[3,35], E. Serradilla[10,63], A. Sevcenco[58], A. Shabanov[52], A. Shabetai[113], O. Shadura[3], R. Shahoyan[35], M.I. Shahzad[16], A. Shangaraev[111], A. Sharma[91], M. Sharma[91], M. Sharma[91], N. Sharma[125], A.I. Sheikh[133], K. Shigaki[46], Q. Shou[7], K. Shtejer[9,26], Y. Sibiriak[80], S. Siddhanta[105], K.M. Sielewicz[35], T. Siemiarczuk[77], D. Silvermyr[33], C. Silvestre[71], G. Simatovic[129], G. Simonetti[35], R. Singaraju[133], R. Singh[79], S. Singha[79,133], V. Singhal[133], B.C. Sinha[133], T. Sinha[100], B. Sitar[38], M. Sitta[31], T.B. Skaali[21], M. Slupecki[123], N. Smirnov[137], R.J.M. Snellings[53], T.W. Snellman[123], J. Song[96], M. Song[138], Z. Song[7], F. Soramel[29], S. Sorensen[125], R.D.de Souza[121], F. Sozzi[97], M. Spacek[39], E. Spiriti[72], I. Sputowska[117], M. Spyropoulou-Stassinaki[89], J. Stachel[93], I. Stan[58], P. Stankus[85], E. Stenlund[33], G. Steyn[65], J.H. Stiller[93], D. Stocco[113], P. Strmen[38], A.A.P. Suaide[120], T. Sugitate[46], C. Suire[51], M. Suleymanov[16], M. Suljic[I,25], R. Sultanov[54], M. Šumbera[84], S. Sumowidagdo[49], A. Szabo[38], I. Szarka[38], A. Szczepankiewicz[35], M. Szymanski[134], U. Tabassam[16], J. Takahashi[121], G.J. Tambave[22], N. Tanaka[128], M. Tarhini[51], M. Tariq[18], M.G. Tarzila[78], A. Tauro[35], G. Tejeda Muñoz[2], A. Telesca[35], K. Terasaki[127], C. Terrevoli[29], B. Teyssier[130], J. Thäder[74], D. Thakur[48], D. Thomas[118], R. Tieulent[130], A. Tikhonov[52], A.R. Timmins[122], A. Toia[60], S. Trogolo[26], G. Trombetta[32], V. Trubnikov[3], W.H. Trzaska[123], T. Tsuji[127], A. Tumkin[99], R. Turrisi[107], T.S. Tveter[21], K. Ullaland[22], A. Uras[130], G.L. Usai[24], A. Utrobicic[129], M. Vala[55], L. Valencia Palomo[70], S. Vallero[26], J. Van Der Maarel[53], J.W. Van Hoorne[35], M. van Leeuwen[53], T. Vanat[84], P. Vande Vyvre[35], D. Varga[136], A. Vargas[2], M. Vargyas[123], R. Varma[47], M. Vasileiou[89], A. Vasiliev[80], A. Vauthier[71], O. Vázquez Doce[36,94], V. Vechernin[132], A.M. Veen[53], M. Veldhoen[53], A. Velure[22], E. Vercellin[26], S. Vergara Limón[2], R. Vernet[8], M. Verweij[135], L. Vickovic[116], J. Viinikainen[123], Z. Vilakazi[126], O. Villalobos Baillie[101], A. Villatoro Tello[2], A. Vinogradov[80], L. Vinogradov[132], Y. Vinogradov[I,99], T. Virgili[30], V. Vislavicius[33], Y.P. Viyogi[133], A. Vodopyanov[66], M.A. Völkl[93], K. Voloshin[54], S.A. Voloshin[135], G. Volpe[32,136], B. von Haller[35], I. Vorobyev[36,94], D. Vranic[35,97], J. Vrláková[40], B. Vulpescu[70], B. Wagner[22], J. Wagner[97], H. Wang[53], M. Wang[7,113], D. Watanabe[128], Y. Watanabe[127], M. Weber[35,112], S.G. Weber[97], D.F. Weiser[93], J.P. Wessels[61], U. Westerhoff[61], A.M. Whitehead[90], J. Wiechula[34], J. Wikne[21], G. Wilk[77], J. Wilkinson[93], M.C.S. Williams[104], B. Windelband[93], M. Winn[93], P. Yang[7], S. Yano[46], Z. Yasin[16], Z. Yin[7], H. Yokoyama[128], I.-K. Yoo[96], J.H. Yoon[50], V. Yurchenko[3], I. Yushmanov[80], A. Zaborowska[134], V. Zaccolo[81], A. Zaman[16], C. Zampolli[35,104], H.J.C. Zanoli[120], S. Zaporozhets[66], N. Zardoshti[101], A. Zarochentsev[132], P. Závada[56], N. Zaviyalov[99], H. Zbroszczyk[134], I.S. Zgura[58], M. Zhalov[86], H. Zhang[22], X. Zhang[7,74], Y. Zhang[7], C. Zhang[53], Z. Zhang[7], C. Zhao[21], N. Zhigareva[54], D. Zhou[7], Y. Zhou[81], Z. Zhou[22], H. Zhu[22], J. Zhu[7,113], A. Zichichi[12,27], A. Zimmermann[93], M.B. Zimmermann[35,61], G. Zinovjev[3], M. Zyzak[42]

Affiliation Notes

[I] Deceased
[II] Also at: Georgia State University, Atlanta, Georgia, United States
[III] Also at Department of Applied Physics, Aligarh Muslim University, Aligarh, India
[IV] Also at: M.V. Lomonosov Moscow State University, D.V. Skobeltsyn Institute of Nuclear, Physics, Moscow, Russia

Collaboration Institutes

[1] A.I. Alikhanyan National Science Laboratory (Yerevan Physics Institute) Foundation, Yerevan, Armenia
[2] Benemérita Universidad Autónoma de Puebla, Puebla, Mexico
[3] Bogolyubov Institute for Theoretical Physics, Kiev, Ukraine
[4] Bose Institute, Department of Physics and Centre for Astroparticle Physics and Space Science (CAPSS), Kolkata, India
[5] Budker Institute for Nuclear Physics, Novosibirsk, Russia
[6] California Polytechnic State University, San Luis Obispo, California, United States
[7] Central China Normal University, Wuhan, China
[8] Centre de Calcul de l'IN2P3, Villeurbanne, France
[9] Centro de Aplicaciones Tecnológicas y Desarrollo Nuclear (CEADEN), Havana, Cuba
[10] Centro de Investigaciones Energéticas Medioambientales y Tecnológicas (CIEMAT), Madrid, Spain
[11] Centro de Investigación y de Estudios Avanzados (CINVESTAV), Mexico City and Mérida, Mexico
[12] Centro Fermi - Museo Storico della Fisica e Centro Studi e Ricerche "Enrico Fermi", Rome, Italy
[13] Chicago State University, Chicago, Illinois, USA
[14] China Institute of Atomic Energy, Beijing, China
[15] Commissariat à l'Energie Atomique, IRFU, Saclay, France
[16] COMSATS Institute of Information Technology (CIIT), Islamabad, Pakistan
[17] Departamento de Física de Partículas and IGFAE, Universidad de Santiago de Compostela, Santiago de Compostela, Spain
[18] Department of Physics, Aligarh Muslim University, Aligarh, India
[19] Department of Physics, Ohio State University, Columbus, Ohio, United States
[20] Department of Physics, Sejong University, Seoul, South Korea
[21] Department of Physics, University of Oslo, Oslo, Norway
[22] Department of Physics and Technology, University of Bergen, Bergen, Norway
[23] Dipartimento di Fisica dell'Università 'La Sapienza' and Sezione INFN Rome, Italy
[24] Dipartimento di Fisica dell'Università and Sezione INFN, Cagliari, Italy
[25] Dipartimento di Fisica dell'Università and Sezione INFN, Trieste, Italy
[26] Dipartimento di Fisica dell'Università and Sezione INFN, Turin, Italy
[27] Dipartimento di Fisica e Astronomia dell'Università and Sezione INFN, Bologna, Italy
[28] Dipartimento di Fisica e Astronomia dell'Università and Sezione INFN, Catania, Italy
[29] Dipartimento di Fisica e Astronomia dell'Università and Sezione INFN, Padova, Italy
[30] Dipartimento di Fisica 'E.R. Caianiello' dell'Università and Gruppo Collegato INFN, Salerno, Italy
[31] Dipartimento di Scienze e Innovazione Tecnologica dell'Università del Piemonte Orientale and Gruppo Collegato INFN, Alessandria, Italy
[32] Dipartimento Interateneo di Fisica 'M. Merlin' and Sezione INFN, Bari, Italy
[33] Division of Experimental High Energy Physics, University of Lund, Lund, Sweden

[34] Eberhard Karls Universität Tübingen, Tübingen, Germany
[35] European Organization for Nuclear Research (CERN), Geneva, Switzerland
[36] Excellence Cluster Universe, Technische Universität München, Munich, Germany
[37] Faculty of Engineering, Bergen University College, Bergen, Norway
[38] Faculty of Mathematics, Physics and Informatics, Comenius University, Bratislava, Slovakia
[39] Faculty of Nuclear Sciences and Physical Engineering, Czech Technical University in Prague, Prague, Czech Republic
[40] Faculty of Science, P.J. Šafárik University, Košice, Slovakia
[41] Faculty of Technology, Buskerud and Vestfold University College, Vestfold, Norway
[42] Frankfurt Institute for Advanced Studies, Johann Wolfgang Goethe-Universität Frankfurt, Frankfurt, Germany
[43] Gangneung-Wonju National University, Gangneung, South Korea
[44] Gauhati University, Department of Physics, Guwahati, India
[45] Helsinki Institute of Physics (HIP), Helsinki, Finland
[46] Hiroshima University, Hiroshima, Japan
[47] Indian Institute of Technology Bombay (IIT), Mumbai, India
[48] Indian Institute of Technology Indore, Indore (IITI), India
[49] Indonesian Institute of Sciences, Jakarta, Indonesia
[50] Inha University, Incheon, South Korea
[51] Institut de Physique Nucléaire d'Orsay (IPNO), Université Paris-Sud, CNRS-IN2P3, Orsay, France
[52] Institute for Nuclear Research, Academy of Sciences, Moscow, Russia
[53] Institute for Subatomic Physics of Utrecht University, Utrecht, Netherlands
[54] Institute for Theoretical and Experimental Physics, Moscow, Russia
[55] Institute of Experimental Physics, Slovak Academy of Sciences, Košice, Slovakia
[56] Institute of Physics, Academy of Sciences of the Czech Republic, Prague, Czech Republic
[57] Institute of Physics, Bhubaneswar, India
[58] Institute of Space Science (ISS), Bucharest, Romania
[59] Institut für Informatik, Johann Wolfgang Goethe-Universität Frankfurt, Frankfurt, Germany
[60] Institut für Kernphysik, Johann Wolfgang Goethe-Universität Frankfurt, Frankfurt, Germany
[61] Institut für Kernphysik, Westfälische Wilhelms-Universität Münster, Münster, Germany
[62] Instituto de Ciencias Nucleares, Universidad Nacional Autónoma de México, Mexico City, Mexico
[63] Instituto de Física, Universidad Nacional Autónoma de México, Mexico City, Mexico
[64] Institut Pluridisciplinaire Hubert Curien (IPHC), Université de Strasbourg, CNRS-IN2P3, Strasbourg, France
[65] iThemba LABS, National Research Foundation, Somerset West, South Africa
[66] Joint Institute for Nuclear Research (JINR), Dubna, Russia
[67] Konkuk University, Seoul, South Korea
[68] Korea Institute of Science and Technology Information, Daejeon, South Korea
[69] KTO Karatay University, Konya, Turkey
[70] Laboratoire de Physique Corpusculaire (LPC), Clermont Université, Université Blaise Pascal, CNRS–IN2P3, Clermont-Ferrand, France
[71] Laboratoire de Physique Subatomique et de Cosmologie, Université Grenoble-Alpes, CNRS-IN2P3, Grenoble, France
[72] Laboratori Nazionali di Frascati, INFN, Frascati, Italy
[73] Laboratori Nazionali di Legnaro, INFN, Legnaro, Italy
[74] Lawrence Berkeley National Laboratory, Berkeley, California, United States
[75] Moscow Engineering Physics Institute, Moscow, Russia
[76] Nagasaki Institute of Applied Science, Nagasaki, Japan
[77] National Centre for Nuclear Studies, Warsaw, Poland
[78] National Institute for Physics and Nuclear Engineering, Bucharest, Romania

[79] National Institute of Science Education and Research, Bhubaneswar, India
[80] National Research Centre Kurchatov Institute, Moscow, Russia
[81] Niels Bohr Institute, University of Copenhagen, Copenhagen, Denmark
[82] Nikhef, Nationaal instituut voor subatomaire fysica, Amsterdam, Netherlands
[83] Nuclear Physics Group, STFC Daresbury Laboratory, Daresbury, United Kingdom
[84] Nuclear Physics Institute, Academy of Sciences of the Czech Republic, Řež u Prahy, Czech Republic
[85] Oak Ridge National Laboratory, Oak Ridge, Tennessee, United States
[86] Petersburg Nuclear Physics Institute, Gatchina, Russia
[87] Physics Department, Creighton University, Omaha, Nebraska, United States
[88] Physics Department, Panjab University, Chandigarh, India
[89] Physics Department, University of Athens, Athens, Greece
[90] Physics Department, University of Cape Town, Cape Town, South Africa
[91] Physics Department, University of Jammu, Jammu, India
[92] Physics Department, University of Rajasthan, Jaipur, India
[93] Physikalisches Institut, Ruprecht-Karls-Universität Heidelberg, Heidelberg, Germany
[94] Physik Department, Technische Universität München, Munich, Germany
[95] Purdue University, West Lafayette, Indiana, United States
[96] Pusan National University, Pusan, South Korea
[97] Research Division and ExtreMe Matter Institute EMMI, GSI Helmholtzzentrum für Schwerionenforschung, Darmstadt, Germany
[98] Rudjer Bošković Institute, Zagreb, Croatia
[99] Russian Federal Nuclear Center (VNIIEF), Sarov, Russia
[100] Saha Institute of Nuclear Physics, Kolkata, India
[101] School of Physics and Astronomy, University of Birmingham, Birmingham, United Kingdom
[102] Sección Física, Departamento de Ciencias, Pontificia Universidad Católica del Perú, Lima, Peru
[103] Sezione INFN, Bari, Italy
[104] Sezione INFN, Bologna, Italy
[105] Sezione INFN, Cagliari, Italy
[106] Sezione INFN, Catania, Italy
[107] Sezione INFN, Padova, Italy
[108] Sezione INFN, Rome, Italy
[109] Sezione INFN, Trieste, Italy
[110] Sezione INFN, Turin, Italy
[111] SSC IHEP of NRC Kurchatov institute, Protvino, Russia
[112] Stefan Meyer Institut für Subatomare Physik (SMI), Vienna, Austria
[113] SUBATECH, Ecole des Mines de Nantes, Université de Nantes, CNRS-IN2P3, Nantes, France
[114] Suranaree University of Technology, Nakhon Ratchasima, Thailand
[115] Technical University of Košice, Košice, Slovakia
[116] Technical University of Split FESB, Split, Croatia
[117] The Henryk Niewodniczanski Institute of Nuclear Physics, Polish Academy of Sciences, Cracow, Poland
[118] The University of Texas at Austin, Physics Department, Austin, Texas, USA
[119] Universidad Autónoma de Sinaloa, Culiacán, Mexico
[120] Universidade de São Paulo (USP), São Paulo, Brazil
[121] Universidade Estadual de Campinas (UNICAMP), Campinas, Brazil
[122] University of Houston, Houston, Texas, United States
[123] University of Jyväskylä, Jyväskylä, Finland
[124] University of Liverpool, Liverpool, United Kingdom
[125] University of Tennessee, Knoxville, Tennessee, United States
[126] University of the Witwatersrand, Johannesburg, South Africa

[127] University of Tokyo, Tokyo, Japan
[128] University of Tsukuba, Tsukuba, Japan
[129] University of Zagreb, Zagreb, Croatia
[130] Université de Lyon, Université Lyon 1, CNRS/IN2P3, IPN-Lyon, Villeurbanne, France
[131] Università di Brescia
[132] V. Fock Institute for Physics, St. Petersburg State University, St. Petersburg, Russia
[133] Variable Energy Cyclotron Centre, Kolkata, India
[134] Warsaw University of Technology, Warsaw, Poland
[135] Wayne State University, Detroit, Michigan, United States
[136] Wigner Research Centre for Physics, Hungarian Academy of Sciences, Budapest, Hungary
[137] Yale University, New Haven, Connecticut, United States
[138] Yonsei University, Seoul, South Korea
[139] Zentrum für Technologietransfer und Telekommunikation (ZTT), Fachhochschule Worms, Worms, Germany